Inhalation Toxicology, 15:761–780, 2003

ISSN: 0895–8378 print / 1091–7691 online
DOI: 10.1080/08958370390217837

Taylor & Francis
healthsciences

PHYSIOLOGIC RESPONSES OF SHEEP TO TWO DIFFERENT METHODS OF PAPAIN EXPOSURE

Andrew Hoffman

Department of Clinical Sciences, Tufts University School of Veterinary Medicine, North Grafton, Massachusetts, USA

A. Courtney Henderson

Department of Biomedical Engineering, Boston University, Boston, Massachusetts, USA

Larry Tsai, Edward Ingenito

Brigham and Woman's Hospital, Harvard University, Boston, Massachusetts, USA

Human emphysema is a progressive, destructive lung disease that produces morphologic and functional heterogeneity throughout its course. Consequently, the mature form of the disease is described by a broad range of anatomic, radiological, and physiologic patterns. This report describes the development and characterization of a sheep model of emphysema that represents many of the essential features of both homogeneous and heterogeneous emphysema. Emphysema was produced by two different techniques of papain exposure: (1) aerosol (75 IU/kg) given weekly for 4 treatments (HM) or (2) aerosol (75 IU/kg) weekly for 3 treatments following subsegmental intrabronchial instillations, 75 IU (in 10 saline) per lobe in 6 lobes (HT). Dexamethasone (0.06 mg/kg iv) was administered prior intrabronchial instillations only. On computed tomography, the HM group had homogeneous emphysema, the HT group gross nonuniformity of disease and bullae formation. Both groups demonstrated a significant ($p < .05$*) increase in residual volume (HM, +38%; HT, +30%). There was a significant increase (*$p = .002$*) in total lung capacity per kilogram for the HM group. Emphysema had no effect on active or passive chest wall compliances. Diffusion capacity was significantly (*$p < .05$*) reduced in both groups. Both elastic (*$p = .066$*) and resistive (*$p = .025$*) components of impedance were increased in the HT, and airway resistance increased significantly in the HM groups. The HM model demonstrated gas trapping, a characteristic feature of emphysema, but failed to replicate the alterations in lung dynamics observed in the human form of this disease. The HT model demonstrated less static hyperinflation but significant frequency dependence and hence appeared to better represent the dynamic characteristics of human emphysema.*

Emphysema has been widely modeled in animals (Karlinsky & Snider, 1978; Mauderly, 1984; Snider et al., 1986, 2002) to study specific pathophysiologic or pathobiologic features of human emphysema (Criner et al., 1999; Corne, 2002). Small animal models have allowed us understand discreet phenomena. For example, guinea pigs exposed to cigarette smoke

Received 25 October 2002; sent for revision 10 December 2002; accepted 5 February 2003.
Funded by NHBL 06226603A1 and Bistech, Inc.
Address correspondence to Andrew M. Hoffman, Associate Professor, Department of Clinical Sciences, Tufts University School of Veterinary Medicine, 200 Westboro Rd, North Grafton, MA 01536, USA. E-mail: andrew.hoffman@tufts.edu

have provided conclusive evidence that smoking leads to alveolar destruction, sufficient to cause flow limitation (Wright & Churg, 1992). However, these animals demonstrate little airway disease, and only small changes in lung physiology. Rats have been employed to study almost every aspect of emphysema, including cellular (macrophage, neutrophil) kinetics, role of metalloproteinases, oxidants, ultra-fine particles, mineral dusts, wood smoke, starvation, barotraumas, and cigarette smoke (Snider et al., 2002). Hamster and mouse models have also been used to explore the destructive effects of enzymes such as elastases and collagenases on lung and diaphragmatic mechanics (Karlinsky et al., 1976; Snider & Sherter, 1977; Lucey et al., 1982; Oliven et al., 1986), and the molecular pathways of emphysema initiation, in particular the role of cytokines (Snider et al., 2002). However, often due to the lack of detailed physiologic studies, their relevance to the clinical condition has been difficult to assess.

Large animal models (dogs, pigs, sheep) have had a significant and complimentary role to play in the study of emphysema, particularly since they facilitate a more detailed approach to physiologic assessment in vivo. For example, the dog has been extremely important in the measurement of closing capacity (Hachenberg et al., 1989; Meyer et al., 1991), choke points (Mink, 1984), structural–functional correlations (Shiraishi et al., 1989), static interactions between adjacent lungs in unilateral disease (Margulies et al., 1992), diaphragm mechanics (Hubmayr et al., 1993), and the distribution of pleural pressures (D'Angelo, 1976). The larger animal makes interventional studies more feasible, such as the study of surgical (Brenner et al., 1998; Chen et al., 1998; Huh et al., 1998) and nonsurgical (bronchoscopic) lung volume reduction (Ingenito et al., 2001). At present, however, none of these large animal models exhibit certain key features of human emphysema, such as frequency dependence of resistance and elastance, heterogeneous morphology, and gas trapping. This has prompted us to develop a large animal model of emphysema with demonstrable structural and functional heterogeneity, while retaining relevant static features of emphysema. In this study, we compared two very specific techniques to induce emphysema in sheep: (1) a uniform (HM) emphysema induced by exposure of sheep to papain aerosols, as we previously described (Ingenito et al., 2001), and (2) a nonuniform (HT) model by exposure to both aerosols and a single bronchoscopically guided instillation of papain to several lung lobes. We hypothesized that a nonuniform distribution of papain would increase functional heterogeneity (i.e., frequency dependence of tissue resistance or elastance) that is not evident in the uniformly exposed group. A second aim of the study was to increase the relevance and improve the interpretative nature of the static and dynamic data. We determined lung volume subdivisions (residual volume, RV; total lung capacity, TLC) using the Campbell diagram that considers static volumes as a function of force balances. Dynamic mechanics was assessed using a high-fidelity system of oscillometry that allows one to partition the contributions of airways and tissues to pulmonary resistance and elastance

(Lutchen et al., 1993). The static and dynamic mechanics in each model were examined for the effect of emphysema, and the results compared for the HM and HT groups.

MATERIALS AND METHODS

Animals

All protocols employed in this study were approved by the Institutional Animal Care and Use Committee at Tufts University. Twelve mixed-breed female sheep aged 2–5 yr were employed. At the beginning of the study, they were dewormed with ivermectin (200 μg/kg im) and vaccinated for tetanus and overeating disease, while given 2 wk of acclimation. During the study period they were fed high-quality grass hay ad libitum.

Study Protocol and Induction of Emphysema

Two studies (Phase 1 and 2) were performed in sequence. In the first phase, we induced a uniform ("homogeneous," abbreviated HM) emphysema (n = 6, 59–87 kg body weight) and in the second phase, we intended to induce a nonuniform ("heterogeneous," abbreviated HT) emphysema in a separate group of sheep (n = 6, 49–70 kg body weight). The experiments were performed at separate time periods (within 1 yr). The order of procedures for the HM sheep was as follows: (1) baseline physiologic measurements, followed 1 wk later by (2) the first of 4 weekly papain (papain aqueous solution, Sigma Chemicals, St. Louis, MO) aerosol exposures (75 IU/Kg body weight diluted 1:1 with physiologic saline), and (3) outcome measures of physiology at 1 mo after final papain exposure. For the HT group, we performed baseline physiology, followed 1 wk later by intrabronchial instillations of papain (75 IU per lobe, diluted to 10 ml with saline), followed 2 wk later by the first of 3 weekly aerosol papain exposures as described for the HM group. To perform aerosolizations, we used two parallel-jet nebulizers (LC Plus, Pari, Midlothian, VA), powered by compressors (ProNeb Turbo, Midlothian, VA) that produced fine (mass median diameter 2 μm) particles. We instilled papain bronchoscopically in the same lobes in all sheep. If numbered as successive branches off the left and right mainstem bronchi (odd numbers are lateral and even numbers medial branches), these included left 1, 3, and 7, and right 4, 6, and 10. Injections were performed through a bronchoscope (GIF N30, Olympus, Tokyo) with 5 mm outside diameter and 90 cm working length. To prevent morbidity and mortality associated with the intrabronchial instillations of papain (HT sheep) we treated the sheep with dexamethasone (0.06 mg/kg iv) immediately prior to the intrabronchial instillations only. The protocol for anesthesia and physiologic measurements included the following: induction with ketamine (7.5 mg/kg iv) and valium (0.3 mg/kg iv), permitting bronchoscopically guided intubation, measurement of functional residual capacity (FRC) and active chest wall compliance during spontaneous breathing efforts

against a closed shutter, followed by relaxation and deeper anesthesia using propofol (50 μg/kg/min iv) for passive lung and chest wall compliance measurements, diffusion capacity, and oscillometry (OVW).

Measurement of Lung Volumes, Pressure–Volume Data for the Lung and Chest Wall, and Carbon Monoxide Diffusion Capacity

Sheep were anesthetized and placed on a cart in supine position with the abdomen positioned over a large (30 cm diameter) cut-out to minimize visceral pressure on the diaphragm. Functional residual capacity (FRC) was measured immediately (within 10 min) after anesthetic induction while the sheep was spontaneously breathing within a whole-body plethysmograph. The plethysmograph, purpose-built out of ½-in Lucite stock (Buxco Electronics, Sharon, CT), included a main chamber (1372 L), which accommodated the sheep cart, and a small reference (P_{atm}) chamber (23.2 L). The main chamber pressure (P_{box}) was calibrated with respect to a known volume of injected air (V_{box}, 30 ml), and the calibration was verified with subsequent step and reciprocal injections (0.5–2 Hz) of air. Box pressure was measured using a low-pressure range (±10 cm H_2O) transducer (SCXL004, Invensys Sensor Systems, Milpitas, CA) and preamplifier (Max2270, Buxco Electronics, Sharon, CT), with the transducer referenced to a second chamber equilibrated with atmosphere ($\tau \approx 10$ s). A differential pressure transducer (Validyne DP45-28, Northridge, CA, ±56 cm H_2O) was used for airway and pleural pressure measurements, and the signal conditioned with a carrier demodulator amplifier (Max2215, Buxco Electronics, Sharon, CT), and commercial data acquisition system (Biosystem XA, Buxco Electronics, Sharon, CT) was used with sampling rate set at 100 Hz. At end-expiration, visible on the trace, we activated an occlusion shutter (model 4285 Pneumatic Shutter, Hans Rudolph, Kansan City, MO) positioned at the oral end of the endotracheal tube. Sheep made inspiratory efforts (<0.5 Hz) against the shutter, permitting measurement of peak changes in airway opening pressure (P_{ao}) relative to V_{box} to derive FRC using the methods of Dubois (DuBois et al., 1956): FRC (liters) = $[(\delta V_{box}/\delta P_{ao} \times (P_B - P_{H_2O})]$. Supplemental anesthesia was used to reduce these efforts if necessary. To correct for drift in V_{box}, we used the average between the absolute increase and subsequent decrease from peak V_{box} for at least three efforts. We excluded large efforts ($V_{box} > 40$ ml). The sheep on the cart was then removed from the plethysmograph for measurements of maximum inspiratory pressures (MIP). An esophageal balloon catheter was passed to the level of the mid-thorax to a distance where maximum pleural pressure and minimal cardiac oscillations were visualized during spontaneous breathing. Pleural pressure ($P_{es} - P_{atm}$) was recorded continuously before and after occlusions at (1) end-expiration at FRC and (2) FRC plus 1–2 L (static volume that produced 8–10 cm H_2O pleural pressure). The maximum inspiratory pressure (MIP) was defined as the presence of 3 successive efforts with pressures within 10% of each other or declining. In general, this required from 30 to 90 s of occlusion. Two data points (MIP_{FRC} or MIP_{FRC+X})

were used to construct a slope and intercept that described the active chest wall compliance for each sheep. These were averaged to obtain group compliance for plotting on the Campbell diagram (described later). Sheep were then started on the propofol infusion and mechanical ventilation (V_T 10 ml/kg, f 12/min, FIO_2 0.6, PEEP 0 cm H_2O), which was interrupted only for static and dynamic measurements. Pulse oximetry was employed for continuous monitoring of heart rate and hemoglobin saturations (SaO_2). Deflation pressure–volume curves were generated using a precision volume syringe (3L calibration syringe, Hans Rudolph, Kansas City, MO) and recordings of respective transpulmonary (Ptp = $P_{esophageal} - P_{tracheal}$) pressure. Following at least two large inflations (20 ml/kg) to establish volume history, the lung was inflated from FRC to a minimum of 30 cm H_2O, and pressure was recorded at each deflation step (0.25 L and 4 s per step), until the syringe was emptied; typically there were 7–10 steps. The average pressure–volume data points from two runs for each sheep were fit to the exponential Salazar–Knowles equation by visual inspection (Salazar & Knowles, 1964; Collie, 1994):

$$V(P) = V_{max} - Ae^{-kP},$$

where k is the exponential curve "shape factor," V_{max} the volume at "infinite" distending pressure, V_{min} the residual volume (RV), and A the volume difference ($V_{max} - V_{min}$). For positioning of the pressure–volume curves, we used the FRC for the individual sheep and the mean transpulmonary pressure for the group (at each period) as a frame of reference. The group mean values for k, V_{max}, and V_{min} for each period were used to plot pressure–volume data on Campbell diagrams.

Passive chest wall pressure–volume data were obtained using the precision syringe for inflation, and pressure was recorded during steps of deflation, starting at maximum inflation of 10 cm H_2O, to –4 to –8 cm H_2O pleural pressure, in 0.5-L increments. The linear slope and intercept for each chest wall (active and passive) pressure–volume data set were computed. Lung and the passive and active chest wall mechanics were plotted as a Campbell diagram (Campbell, 1958; Agostoni & Hyatt, 1986). Group means for the slope and intercept of chest wall compliances (active and passive) were used for plotting. Total lung capacity (TLC) was derived from the intersection of the active chest wall and lung compliance curves.

We measured DL_{co} using the single-breath determination method (Collie et al., 1993), and corrected the measurements for alveolar volume, determined by closed-circuit single-breath helium dilution (Collie et al., 1993). The circuit was previously calibrated with test gas (10% He, 0.3% CO, 21% O_2, and 68.7% N_2) to ±0.1%, and corrected for FIO_2 of 60% and BTPS. We used the measured inspired and expired plateau values in a calculation of DL_{co} as follows: $DL_{co} = [V_A/(P_b - P_{H_2O}) \times 60\ s/10\ s \times \ln(Fi_{A_{co}}/Ff_{A_{co}})$, where V_A was the alveolar volume computed from helium dilution.

Oscillometry—Airway and Tissue Mechanics

Low-frequency impedance was measured using the optimal waveform ventilation method (Lutchen et al., 1993) to study input impedances at the following frequencies (Hz): 0.1562, 0.39062, 0.85938, 1.48438, 2.42188, 4.60938, and 8.04688. Tests were performed at a mean airway pressure of 5 cm H_2O, and tidal volume was set at 7 ml/kg. Pulmonary resistance (R_L) and elastance (E_L) were obtained from the real and imaginary portions of impedance, respectively. Pressure-flow data were further fitted to the constant-phase model of the lung (Hantos et al., 1990), from which the input impedance is described according to the following expression:

$$Z(f) = R_{aw} + i2\pi f I_{aw} + G_{ti} - iH_{ti}/(2\pi f)^{\alpha}$$

where $Z(f)$ is the low-frequency input impedance, R_{aw} is airway resistance, I_{aw} is airway inertance, G_{ti}, is tissue damping, H_{ti} is tissue elastance, and α is the exponential relating G_{ti} to H_{ti}:

$$\alpha = (2/\pi) \arctan(H_t/G_t)$$

The term ($R_{aw} + i2\pi f I_{aw}$) described airway impedance, whereas the term $G_{ti} - iH_{ti}/(2\pi f)^{\alpha}$ described the impedance of tissue (Hantos et al., 1990; Petak, 1993; Lutchen et al., 1996). Finally, resonant frequency was measured conventionally as the input frequency coinciding with a reactance value of zero.

Statistical Analysis

The two experimental groups were studied at different time periods. Hence, we tested the effect of papain ("period effect") separately in each group using the paired *t*-test (one-tailed), as well as the effect of "period" and "group" and period × group interaction using a general linear model analysis of variance (ANOVA) (SPSS, Chicago). The following physiological variables were analyzed in this fashion; k, V_{max}, V_{min} (= RV), DL_{co}, DL/V_A, R_{aw}, I_{aw}, G_{ti}, H_{ti}, lung volumes (FRC, RV, TLC, VC from TLC-RV, ERV from FRC-RV, and RV/TLC), and linear descriptors (slopes, intercepts) of the active and passive chest wall data. The frequency of bullae formation was compared for the HM and HT groups using Fisher's exact test. Otherwise, examples of CT images were provided for descriptive purposes only. The histology of the lung was not available since all animals subsequently underwent lung volume reduction prior to euthanasia.

RESULTS

Clinical Response and CT

In the HM group, body weight decreased in four and increased in two sheep, with no significant change (pre 74 ± 0.4 kg; post 72.5 ± 0.4 kg) for

the group. In contrast, we observed mild weight loss, from 58.8 ± 0.35 to 56.5 ± 0.34 kg, in the HT group (p = .03). There was no difference in weight change between HM and HT. In none of the animals did we observe clinical signs of respiratory disease, with the exception of two sheep in the HT group (numbers 116 and 0037) in which periodic cough was observed.

The typical appearance of the HM and HT sheep on CT is depicted in Figure 1. In the HM group, emphysema was characteristically uniform in contrast to the marked nonuniformity of emphysematous changes. None of the sheep in the HM group developed emphysematous bullae visible on CT, whereas four of six sheep in the HT group developed at least one large (>2 cm^2) bullae ($p < .001$).

Lung Volumes, Static Mechanics, and Diffusion Capacity

Functional residual capacity increased significantly (p = .005) in the HM group (Table 1), from 1.78 ± 0.075 to 2.1 ± 0.01 L (+18%). Residual volume (V_{min}) increased significantly ($p < .05$) in both HM (+38%) and HT (+30%) groups (Tables 1 and 2). Normalized to initial body weight, there were significant increases in RV (p = .024) and FRC (p = .007) for the HM group, and an increase in RV (p = .024) and RV per kilogram body weight (p = .01) in the HT group. The computed ERV was significantly (p = .013) decreased in the HT group, from 0.615 ± 0.098 L to 0.408 ± 0.084 L. In contrast, there was no change in ERV for the HM group (pre 0.835 ± 0.075 L, post 0.800 ± 0.162 L).

The pressure–volume curves for both groups were shifted upward and toward the volume axis (Figure 2) largely due to changes in FRC, but there

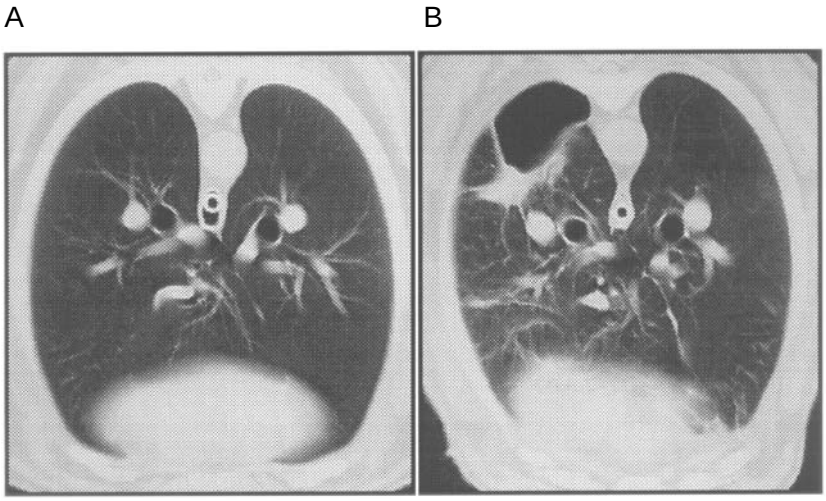

FIGURE 1. Representative examples of mid-lung CT of (A) an HM sheep (9912) and (B) an HT sheep (0037). In the HM sheep there was uniformity and mild emphysematous changes on CT. In contrast, the HT sheep exhibited gross nonuniformity of disease, including bullae and irregular foci of emphysema and increased density (i.e., fibrosis) associated with sites of bronchoscopic instillation.

TABLE 1. Lung volumes derived using plethysmography (FRC), from the Campbell diagrams (TLC, VC), or Salazar–Knowles exponential model of the static pressure–volume data for the lung (k, V_{max}, and V_{min}, i.e., RV) for the homogeneous emphysema (HM) group before and after papain

Sheep	Period	FRC	TLC	VC	RV/TLC	k	V_{max}	V_{min}
3	Pre	1.78	2.90	2.00	0.31	0.22	3.20	0.90
9912	Pre	1.53	3.04	2.44	0.20	0.15	3.50	0.60
9712	Pre	1.73	3.80	3.10	0.18	0.16	4.00	0.70
9721	Pre	2.05	3.45	1.95	0.43	0.12	3.50	1.50
24	Pre	1.78	3.45	2.55	0.26	0.15	4.00	0.90
50	Pre	1.84	2.78	1.68	0.40	0.15	3.10	1.10
	Mean	1.79	3.24	2.29	0.30	0.16	3.55	0.95
	SEM	0.08	0.18	0.23	0.05	0.01	0.17	0.14
	CV (%)	9.42	12.12	22.45	34.59	21.03	10.80	33.78
3	Post	2.21	3.58	2.58	0.28	0.20	4.40	1.00
9912	Post	2.09	3.38	2.03	0.40	0.15	3.60	1.35
9712	Post	1.93	3.78	2.78	0.26	0.16	4.10	1.00
9721	Post	2.50	3.62	1.42	0.61	0.09	3.80	2.20
24	Post	1.99	3.66	2.86	0.22	0.18	4.20	0.80
50	Post	1.88	2.75	1.30	0.53	0.15	2.85	1.45
	Mean	2.10	3.46	2.16	0.38	0.16	3.83	1.30
	SEM	0.11	0.18	0.33	0.07	0.02	0.24	0.24
	CV (%)	11.84	11.88	33.88	43.43	21.69	14.03	41.37
	p	.011	.091	.531	.098	.781	.227	.049

Note. Lung volumes are expressed in liters.

was also a trend (p = .065) toward a significant increase in k for the HT group that contributed to this change (Table 2). The volume at infinite inflation (V_{max}) was increased in five of the six HM sheep, but the effect was more variable in the HT group, with three showing an increase and three a decrease in V_{max}. In neither group was V_{max} found to change significantly.

There was no statistical change in TLC, unless this variable was normalized to initial body weights, whereby it increased significantly (p = .047) in the HM group. There were trends noted towards a significant increase in the RV to TLC ratio for the HM (p = .097) and HT (p = .065) groups.

The pressure–volume data (slopes, intercepts) for the chest wall and maximum inflation pressures generated by active chest wall and diaphragmatic contractions were unchanged with papain administration (Table 3).

Diffusion capacity (DL_{co}) and DL_{co} as a function of V_A (DL/V_A), decreased significantly ($p < .05$) for both groups; the decrease in DL_{co} and DL/V_A for the homogeneous group was 35% and 35%, respectively and for the heterogeneous group was 37% and 51%, respectively (Figure 3).

Oscillometry

In the HM, there was a significant increase in R_{aw}, which uniformly shifted the R_L versus frequency plot for the group, upwards (Figure 4). In

TABLE 2. Lung volumes derived using plethysmography (FRC), from the Campbell diagrams (TLC, VC), or Salazar–Knowles exponential model of the static pressure–volume data for the lung (k, V_{max}, and V_{min}, i.e., RV) for the heterogeneous emphysema (HT) group before and after papain

Sheep	Period	FRC	TLC	VC	RV/TLC	k	V_{max}	V_{min}
115	Pre	1.07	2.64	2.14	0.19	0.12	3.15	0.50
116	Pre	2.26	3.35	1.50	0.55	0.08	4.20	1.85
117	Pre	2.06	3.52	1.97	0.44	0.06	4.45	1.55
118	Pre	2.49	4.10	2.30	0.44	0.10	4.75	1.80
37	Pre	1.32	3.27	2.97	0.09	0.20	3.60	0.30
121	Pre	1.39	2.52	1.62	0.36	0.13	2.90	0.90
	Mean	1.77	3.23	2.08	0.34	0.12	3.84	1.15
	SEM	0.26	0.26	0.24	0.08	0.02	0.33	0.30
	CV (%)	32.87	18.08	25.44	50.10	42.51	19.29	58.72
115	Post	1.40	2.62	1.52	0.42	0.15	2.90	1.10
116	Post	2.55	4.00	1.90	0.53	0.15	4.30	2.10
117	Post	2.55	4.05	1.85	0.54	0.10	4.90	2.20
118	Post	2.06	3.61	1.91	0.47	0.12	4.10	1.70
37	Post	1.66	3.23	2.33	0.28	0.21	4.40	0.90
121	Post	1.17	2.37	1.42	0.40	0.12	2.70	0.95
	Mean	1.90	3.31	1.82	0.44	0.14	3.88	1.49
	SEM	0.26	0.31	0.14	0.04	0.02	0.39	0.26
	CV (%)	30.73	21.25	17.80	22.00	28.26	22.71	39.23
	p	.414	.669	.159	.065	.065	.853	.048

Note. Lung volumes expressed in liters.

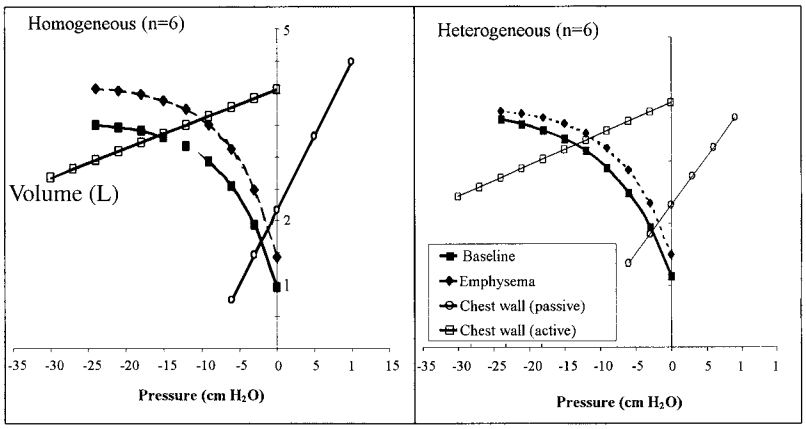

FIGURE 2. Campbell diagrams, including active and passive chest wall compliance, and lung compliance curves before and after papain to create homogeneous (HM) or heterogeneous (HT) emphysema. The diagrams were employed to measure TLC and describe lung–chest wall interactions. In both groups there was a significant ($p < .05$) increase in RV that shifted the curves upward, and a marked increase in TLC per kilogram body weight in the HM group only. There were no changes in chest wall compliances, so the curves are derived from pooled slopes and intercepts for each group.

TABLE 3. Active and passive chest wall pressure–volume data for the homogeneous (HM) and heterogeneous (HT) emphysema groups before (PRE) and after (POST) papain exposures

	Active chest wall				Passive chest wall			
	Slope		Intercept		Slope		Intercept	
Sheep	PRE	POST	PRE	POST	PRE	POST	PRE	POST
Homogeneous emphysema group (n = 6)								
3	0.068	0.035	3.76	3.85	0.496	0.200	1.82	2.50
9912	0.043	0.044	3.63	4.08	0.222	0.140	2.20	2.41
9712	0.021	0.027	4.28	4.31	0.230	0.250	2.56	2.26
9721	0.044	0.050	4.05	5.25	0.300	0.260	2.15	1.68
24	0.063	0.054	4.60	4.19	0.170	0.260	1.80	2.34
50	0.029	0.063	3.22	3.94	0.150	0.110	2.05	2.06
Mean	0.045	0.045	3.92	4.27	0.261	0.203	2.10	2.21
SEM	0.008	0.006	0.22	0.23	0.057	0.029	0.13	0.13
p		.930		.20		.328		.57
Heterogeneous emphysema group (n = 6)								
115	0.036	0.052	2.81	3.32	0.096	0.137	1.65	2.23
116	0.030	0.041	3.76	4.59	0.134	0.162	2.26	2.84
117	0.055	0.041	4.67	4.55	0.169	0.181	2.78	2.99
118	0.055	0.123	4.88	5.26	0.144	0.163	2.49	2.60
37	0.051	0.040	4.03	3.43	0.280	0.150	2.59	1.92
121	0.053	0.031	3.25	2.78	0.116	0.120	1.96	1.67
Mean	0.047	0.055	3.90	3.99	0.156	0.152	2.29	2.38
SEM	0.004	0.014	0.33	0.39	0.027	0.009	0.17	0.21
p		.578		.72		.876		.68

contrast, in the HT group, mean R_{aw} did not change but R_L increased independently at the low input frequencies. This nonuniform behavior of resistance as a function of frequency was reflected quantitatively in a significant (p = .026) increase in the viscous dissipative factor (G_t) for the HT group (Table 4). The dynamic profile for E_L was not significantly altered with respect to input frequency in the HT group, although there were trends toward an increase in H_t (p = .066) and resonant frequency (pre 5.7 ± 1.1 Hz, post 8.2 ± 1.8 Hz, p = .054). In the HM group where there was no change in resonant frequency observed (pre 5.7 ± 0.61 Hz, post 6.2 ± 0.82 Hz, p = .7). The goodness of model fit, as described by the individual and mean σ^2 values, appeared to be equivalent for two groups. There was no effect of group (HM vs. HT) or period (pre–post emphysema) on the oscillometry variables.

DISCUSSION

The principal objective of this study was to develop and characterize a large animal model that adequately expressed the spectrum of physiologic

and radiological features observed in human disease. The sheep was chosen due to its comparable size, similarities in surface area to volume ratios, and with regard to airway branching morphometry with humans. Information pertaining to the use of this species for emphysema research is comparatively lacking in the literature (Janoff et al., 1983; Susskind et al., 1984), so we did not have an expansive base in the literature from which to derive techniques specific to sheep.

Initially we have worked with sheep exposed with papain by inhalation, and induced emphysema that was structurally and functionally homogeneous (Ingenito et al., 2001). In this study, aerosol exposure of the sheep lung to papain resulted in similar changes in lung volumes to that seen in other animal species using aerosols, but mild changes in comparison to humans with severe emphysema that experience an increase in RV of 120–153% (Criner et al., 1999; Geddes et al., 2000). Specifically there was a moderate increase in RV (38%) and FRC (18%), in comparison to changes observed in dogs [FRC +21% (Marco et al., 1972); RV +51% and FRC +20% (Hachenberg et al., 1989); RV +10% and FRC +10% (Shiraishi et al., 1989); FRC +39% (Barnas et al., 1997). Intratracheal or intrabronchial instillations of papain for the most part had a greater effect to increase lung volumes, for example, in dogs, causing increases in RV by 25% (Pushpakom et al., 1970), 77% (D'Angelo, 1976), 91% (Shiraishi et al., 1989), or 140% (Mink, 1984). Similarly, RV or FRC increased to >200% baseline in

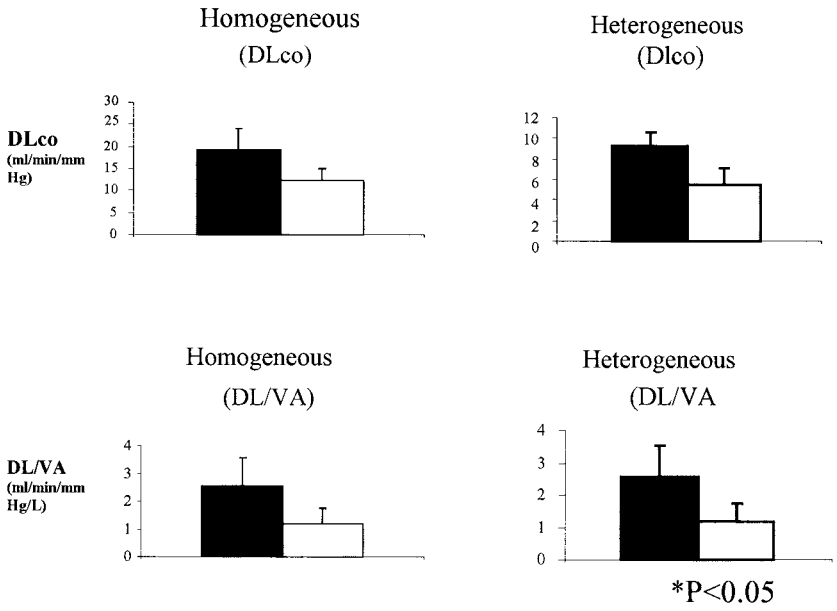

FIGURE 3. Diffusion capacity (DL_{co}) and diffusion capacity as a function of effective alveolar volume (DL/V_A) using the single–breath He dilution method. Significant diffusion limitation was observed in both groups as a function of emphysema.

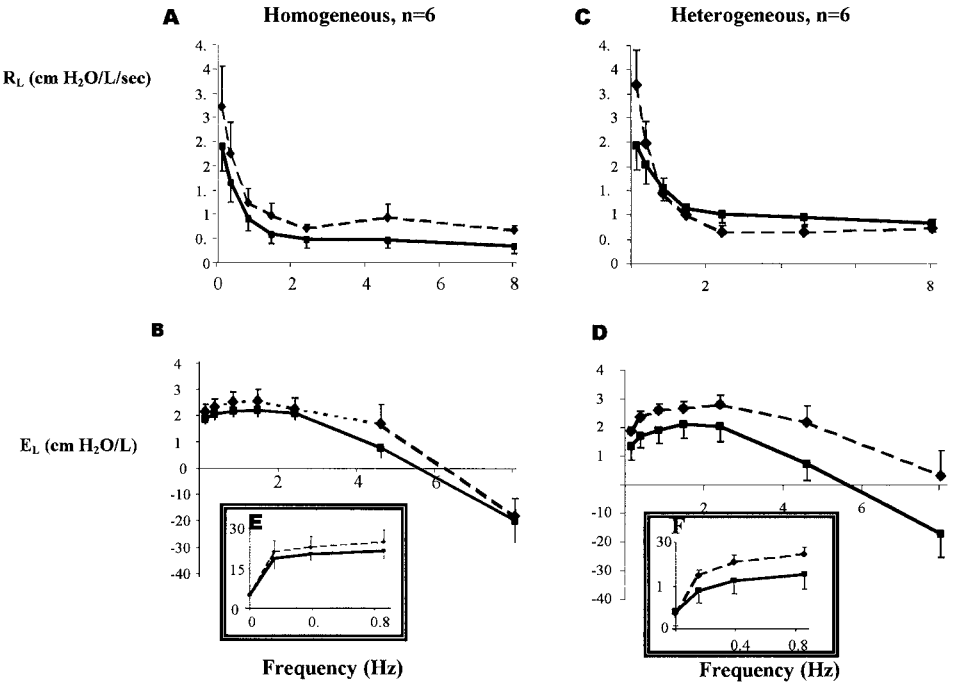

FIGURE 4. Dynamic data from the HM and HT groups differed with respect to frequency dependence of resistance and elastance, as can be seen by the shape and position of the R_L curves. In the HM group, there is a parallel shift upward for R_L as a result of a significant increase in R_{aw}. There was a slight shift upward of the elastance curve but tissue elastance (H_{ti}) was not significantly altered in this model. In contrast, in HT there was a significant increase in frequency dependence of R_L. The El data (enlarged in E and F for HM and HT respectively) for HT shows a more marked increase in frequency dependence. There was a significant ($p < .05$) increase in the resonant frequency for the HT group only.

hamsters in response to intratracheal elastase (Snider & Sherter, 1977; Lucey et al., 1982; Thomas et al., 1986; Sullivan et al., 1998). These changes are more substantial than observed in our HT group with a single papain instillation into six different subsegmental lung lobes, in addition to three aerosolizations (RV +30%, FRC +12%). While causing more severe local pathology, endoscopic injections have the potential to introduce an unacceptable cost of higher morbidity and mortality, particularly where long-term studies involving multiple interventions, and larger species.

The purpose of using exponential analysis of the pressure–volume curves was to (1) better characterize the effect of emphysema over the full range of lung volumes, (2) employ a variable (k) that is independent of TLC and end-expiratory lung volume and body weight (Collie, 1994), and (3) assist in plotting pressure–volume data in the format of a Campbell diagram. In humans with severe emphysema, k increased by 46% in one study (Gibson et al., 1979). In contrast, papain did not alter the shape factor k significantly in either group of sheep, suggesting that the main effect of papain was to alter

lung volumes due to air trapping. There were trends for papain to increase TLC and RV/TLC and cause a decrease in VC. If normalized for starting body weight, TLC increased significantly in the HM group. The normalization to body weight was undertaken in consideration of a previous study that showed a significant correlation between FRC and body weight in

TABLE 4. The low-frequency input impedance was described using the constant phase model of the lung, and a paired *t*-test (two-tailed) was used to test the effect of papain on variables derived from the model within each group

Sheep	Period	R_{aw}	I_{aw}	G_t	H_t	α	σ^2
Homogeneous emphysema group (n = 6)							
3	Pre	0.635	0.0113	1.88	15.4	0.923	0.0055
3	Post	0.399	0.0173	1.3	16.4	0.95	0.0128
9912	Pre	0.136	0.00995	1.97	16.1	0.959	0.0344
9912	Post	0.659	0.0183	1.83	22.3	0.937	0.0465
9712	Pre	0.127	0.0138	1.63	16.3	0.928	0.06
9712	Post	0.583	0.0191	1.9	17	0.923	0.0413
9721	Pre	0.986	0.0315	3.93	22.9	0.937	0.0816
9721	Post	1.51	0.00894	6.04	28.7	0.929	0.243
24	Pre	0.139	0.0223	1.04	16	0.892	0.007
24	Post	0.542	0.0152	1.27	12.8	0.868	0.009
50	Pre	0.0817	0.01442	3.05	26.9	0.922	0.0817
50	Post	0.503	0.0183	3.81	31.5	0.948	0.105
Mean	Pre	0.351	0.0172	2.25	18.93	0.927	0.045
SEM		0.147	0.0032	0.413	1.88	0.009	0.0136
Mean	Post	0.699	0.0162	2.692	21.45	0.926	0.0763
SEM		0.159	0.0015	0.74	2.91	0.0118	0.0348
p		.0324	.841	.298	.153	.927	
Heterogeneous emphysema group (n = 6)							
115	Pre	0.667	0.016	1.24	9.83	0.92	0.019
115	Post	1.34	0.014	3.18	13.3	0.85	0.038
116	Pre	0.597	0.022	3.22	22	0.908	0.082
116	Post	0.656	0.017	3.43	25.6	0.915	0.103
117	Pre	1.31	0.012	1.07	9.1	0.925	0.049
117	Post	0.19	0.011	0.975	6.79	0.909	0.01
118	Pre	0.93	0.0064	3.73	18.6	0.874	0.0495
118	Post	0.361	0.0089	5.48	33.5	0.897	0.0316
37	Pre	0.238	0.0137	1.4	16.3	0.945	0.0745
37	Post	0.407	0.0137	2.67	21	0.919	0.0188
121	Pre	0.997	0.029	1.69	17.9	0.940	0.0912
121	Post	0.294	0.012	3.8	31.4	0.923	0.0263
Mean	Pre	0.7898	0.0163	2.058	15.62	0.919	0.0609
SEM		0.1597	0.0034	0.485	2.203	0.0111	0.011
Mean	Post	0.5413	0.0128	3.256	21.93	0.902	0.038
SEM		0.181	0.0013	0.633	4.474	0.0116	0.0143
p		.40	.269	.025	.066	.263	

Note. R_{aw} (airway resistance), I_{aw} (inertance), G_t (tissue damping), H_t (tissue elastance), and $\alpha = [(2/\pi) \arctan(H_t/G_t)]$.

sheep (Mundie et al., 1992). The lack of significant changes in RV/TLC was presumably due to parallel shifts in RV and TLC, and the small sample size, rather than the nature or severity of pathology.

The pattern of pressure–volume data was different between the HT and HM groups, whereby the pressure–volume curve was shifted upward but quickly formed a plateau, that is, V_{max} in the HT group was unaffected by papain. Disparate patterns of pressure–volume curves for the lung have been observed previously in enzymatic models. For example, Johanson and Pierce (1972), and Karlinsky (Karlinsky et al., 1976), who exposed excised lungs to enzymes, observed decreased elastic recoil but no change in maximum inflation volume. Moreover, Klassen (Klassen et al., 1981) noted dichotomous patterns ("parallel" vs. "skewed" pressure–volume curves) in excised dog lungs exposed to various papain instillations. The HT model represents a more "skewed" pattern per se than that observed for the HM group. The net effect of increasing RV yet minimal change in V_{max} or TLC was a tendency ($p = .065$) toward an increase in the RV/TLC ratio. This effect may be qualitatively more akin to the shrinkage of VC seen in human emphysema. The mechanisms by which HT sheep differ from the HM sheep may relate to the presence of bullae that exert compression on surrounding parenchyma, and express a greater degree of collagen in those areas.

A critical appraisal of our methodologies may shed light on differences between our static data and previous reports using enzymatic destruction to cause emphysema. In reports of past studies, RV was measured using spirometric methods, that is, ERV was obtained by subtraction from FRC, defined by a specific airway pressure causing closure (e.g., –25 cm H_2O). This method is problematic in that the value of RV is confounded by dynamic flow limitation (Rodarte & Rehder, 1986), operator error, and premature airway closure, as well as an arbitrary selection of the pressure endpoint. Hence, it is not a precise representation of static RV. In the current study, RV was determined using exponential analysis of the pressure–volume curve, and absolute position of the curves guided by FRC and associated pleural pressure. This approach may be less prone to dynamic artifacts, since the lung is deflated only to FRC, where an inflection point is generally not observed. The present method might be advantageous to understand the critical factors that determine static RV, when compared with spirometry. The spirometric method of subtraction (i.e., degassing to RV), on the other hand, may result in overestimation of RV and amplify (artificially) the effects of emphysema on static lung volumes.

It is noteworthy that while our method to determined RV has advantages, there are limitations, since it relies on FRC pleural pressure as a frame of reference. The latter measurement is confounded by body position, chest wall tone, compression from mediastinal structures, and the presence of bloat in ruminants. We attempted to reduce variability by making our measurements of FRC immediately after anesthetic induction (reducing bloat), measuring FRC pleural pressure only during deep anesthesia with complete

relaxation (avoiding chest wall effects), and using the group mean pleural pressures. However, a high degree of variation in RV (CV from 33.8 to 41.4%) in comparison to FRC (9.4–11.8%) persisted. This degree of variation is higher than found in some studies of RV using the subtraction method (D'Angelo, 1976; Hachenberg et al., 1989) and lower than others (Shiraishi et al., 1989). This facet was not improved by normalization to body weight. The degree of variation in RV must be accounted for when designing studies involving this animal model.

Total lung capacity was also measured in a fashion that departs from previous animal studies. We imposed an occlusion maneuver at two lung volumes (FRC and FRC + *x* L) and defined TLC as the intersection between the active chest wall and lung compliance curves on the Campbell diagram (Campbell, 1958). The active chest wall compliance curves were reproducible between time periods, and the slopes and intercepts virtually identical between HM and HT groups. This suggests that sheep made consistent maximal inspiratory efforts, albeit under anesthesia, where absolute TLC is probably reduced. The absolute values of V_{max} in our study (mean: HM, 0.048 L/kg; HT, 0.065 L/kg) were similar to those obtained by Collie and coworkers (median 0.065 L/kg), who set their pressure volume curves to TLC by helium dilution (Collie, 1994). In contrast, our values for TLC (determined as a force balance) were lower (HM, 0.044 L/kg; HT, 0.055 L/kg). Hence, our measurements of TLC are at some distance from the flat portion of the pressure–volume curve. More commonly, past researchers have estimated TLC as the inflation volume corresponding to a given raised pressure (e.g., 25–30 cm H_2O). That TLC is not reflective of a balance of static forces per se; rather, it is determined more unilaterally by elastic recoil of the lung, which in turn may be influenced by surface collagen, and extrinsic factors. As TLC at a given pressure is closer to V_{max}, and not as sharply influenced by mid-volume changes in elastance, or the shape of the pressure–volume curve. Hence TLC as a force balance provides some benefit in the analysis of lung compliance over chord compliance measurements (between FRC and FRC + 1.2TLC, for example) that may not change unless there is a major change in slope of the pressure–volume curve.

The effects of emphysema on TLC and V_{max} were qualitatively the same, but only changes in TLC ($p = .09$) or TLC/kg body weight ($p = .002$) showed statistical significance in the HM group; V_{max} did not. This demonstrates the potential value of measuring TLC (vs. V_{max}) as a force balance using the Campbell diagram (Campbell, 1958). To the author's knowledge, this represents the first complete use of the Campbell diagram to measure lung volume subdivisions in animals. Past researchers have plotted lung and chest wall data (Margulies et al., 1992), and even maximal (spontaneous) transdiaphragmatic pressure–volume data (Oliven et al., 1986) during emphysema, with slightly difference purposes in mind. The Campbell diagram allows one to inspect all static forces simultaneously, and may improve our understanding of perturbations in that respect.

Emphysema did not alter passive chest wall mechanics in this study. In contrast, passive recoil was reduced (i.e., chest pressure–volume intercept, not slope, was increased) in golden hamsters exposed to elastase (Thomas et al., 1986). The difference may relate to the greater severity of emphysema created in the hamster, with an increase of FRC to 239% baseline versus 118% in this study, as well as marked differences in the intrinsic chest wall compliances of rodents (higher and more plastic) versus large animals. Active chest wall compliance (slope, intercept) similarly did not change as a consequence of emphysema in either group. Since we used a small group of sheep, we may have missed subtle changes in chest wall mechanics.

In addition to lung volumes and static lung and chest wall mechanics, we measured diffusion capacity (DL_{co}) and corrected DL_{co} (i.e., DL_{co}/V_A). Consistent with previous reports (Collie et al., 1993), we found the measurements to be highly reproducible between animals. The absolute values in this study are much lower than previously reported by Collie and coworkers as they collected alveolar gas, and we measured the change in CO concentrations in mixed gas recovered from the lung The effects of emphysema on DL_{co} and DL/V_A, were similar for the HM (35 and 35%, respectively) and HT (37 and 51%, respectively) groups. This decline denotes a significant loss of alveolar surface area for gas exchange, although the decrease was greater in dogs (–55%), hamsters (–55%), and humans (–40 to –71%) with emphysema (Mauderly, 1984; Criner et al., 1999; Geddes et al., 2000). One might conclude that the effect on diffusion capacity was compatible with moderate emphysema compared to humans.

A number of excellent reviews of animal models of emphysema (Port et al., 1977; Karlinsky & Snider, 1978; Busch et al., 1984; Mauderly, 1984; Snider et al., 1986; Szelenyi & Marx, 2001; Snider et al., 2002) have stressed that the loss of uniform alveolar pattern is similar to human panlobular emphysema at the histologic level. The major differences between animal and human disease are twofold: (1) the lack of airway pathology in animals, with exception where mild bronchiolitis has been specifically induced (Niewoehner & Kleinerman, 1973), and (2) emphysema in animals is more often induced uniformly at the macroscopic level, due to the lack of site-directed techniques. Aerosols and intratracheal instillations presumably distribute uniformly and presumably produce a functionally homogeneous lesion (D'Angelo, 1976), although intratracheal instillations certainly have the potential to distribute nonuniformly depending on body position and ventilatory pattern. Alternatively, intrabronchial (Mink, 1984) or unilateral instillations (Takaro, 1978; Margulies et al., 1992) have the potential to create structural and functional heterogeneity. However, is unclear how this pattern of exposure affects dynamic function. This is relevant from the modeling perspective, as excised lung tissue from humans with emphysema demonstrates an increase in frequency dependence associated with increased peripheral tissue resistance (Verbeken et al., 1992), and humans with chronic obstructive pulmonary disease demonstrate a pattern of fre-

quency dependence of resistance and elastance (Kaczka et al., 2001). In contrast, in animals it has been difficult to produce evidence of heterogeneity. Niewoehner and Kleinerman (1973) induced bronchiolitis and/or emphysema in hamsters and found that emphysema alone was responsible for frequency dependence of compliance. Haddad (Haddad et al., 1979) measured impedance (0.9–16 Hz) in dogs, aerosolized papain, and also noted a change in the frequency dependence of dynamic compliance, and a dependence of resistance on airway pressure level, suggesting peripheral airway disease may contribute to serial or parallel heterogeneity in that model. Measurements of heterogeneity with improved fidelity have evolved, allowing one to separate the measurements of tissue and airway resistance (Lutchen et al., 1993, 1996; Lutchen & Gillis, 1997). Applying these methods with airway and constant–phase tissue modeling (Hantos et al., 1990; Petak et al., 1993), we were previously unable to detect heterogeneity in terms of G_{ti} or H_{ti} in a sheep model, equivalent to the HM group (Ingenito et al., 2001). Similarly, Barnas (Barnas et al., 1997) measured dynamic resistance and elastance using quasi-sinusoidal waveforms over the spontaneous breathing frequency in closed- and open-chested dogs exposed to papain aerosol, and found no change in frequency dependence of resistance and elastance. In this study, we were able to observe a systematic difference in the HM and HT groups with respect to dynamic behavior. There was a significant increase in G_{ti} (tissue dissipation), which reflects frequency dependence of resistance, and a trend toward an increase in H_{ti} (frequency dependence of tissue elastance). These changes may be interpreted as evidence for parallel inequalities in time constants and/or serial heterogeneity (inflated peripheral versus central airway resistance) caused by the papain injections. The former explanation brings together the accentuated regional tissue destruction, with previous evidence that peripheral airways are largely spared with papain exposure in animals (Snider et al., 1986). Caution, however, is warranted in excluding the contribution of airways inflammation or mucus accumulation to dynamic behavior in our models. The HM group demonstrated an increase in airway resistance (R_{aw}) without an increase in frequency dependence. This pattern suggests that papain may elicit inflammation, constriction, or remodeling of central airways, which is not surprising considering the high level of deposition of papain that occurs by aerosolization.

Based on the observation of bullae in several sheep after a single bronchoscopic instillation, we can not recommend repeated bronchoscopic instillations of papain at the current dose (75 units per subsegmental lung lobe), since the safety of repeated injections is unknown. In pilot studies, we found that larger doses (1000 IU per lobe) proved fatal and lower doses (75–300 IU/lobe) were survived, and equally effective to induce bullae and heterogeneous disease (unpublished observations). In part, our use of pretreatment with dexamethasone may have reduced the acute inflammatory or anaphylactic episodes in our sheep, but we have no evidence of that. In a previous study, the use of dexamethasone (Szelenyi & Marx, 2001) or

antineutrophil serum (Kuhn et al., 1980), actually increased the severity of emphysema in hamsters (Snider et al., 1986). Although we did not intend to worsen the emphysema by pretreatment, it is not possible to exclude that dexamethasone somehow modified the response.

In conclusion, there were functional consequences related to the method of producing emphysema in sheep. Both groups possessed equivalent changes in RV and diffusion capacity, but differed qualitatively with respect to TLC, RV/TLC, and most significantly, dynamic airway and tissue function (G_{ti}, H_{ti}, resonant frequency). There was no attempt to study the temporal aspects of these findings, so future work must be directed at following these sheep over longer periods of time. It is important to consider the effects of agent distribution (uniform, nonuniform) on dynamic and static lung function, since these will likely determine the value of the model for the study of specific physiological interventions.

REFERENCES

Agostoni, E., and Hyatt, R. E. 1986. Static behavior of the respiratory system. In *Handbook of physiology,* ed. A. P. Fishman, vol. 3, pp. 113–130. Bethesda, MD: American Physiological Society.

Barnas, G. M., Delaney, P. A., Gheorghiu, I., Mandova, S., Russell, R. G., Kohn, R., and MacKenzie, C. F. 1997. Respiratory impedances and acinar gas transfer in a canine model for emphysema. *J. Appl. Physiol* 83(1):179–188.

Brenner, M., Katie, F. E., Huh, J., Yoong, B., Budd, M., Chen, J. C., Waite, T. A., Mukai, D., Wang, N. S., McKenna, R., Fischel, R., Gelb, A., Wilson, A. F., and Berns, M. W. 1998. Effect of lung volume reduction surgery in a rabbit model of bullous lung disease. *J. Invest. Surg.* 11(4):281–288.

Busch, R. H., Buschbom, R. L., and Smith, L. G. 1984. Comparison of methods for evaluation of experimentally induced emphysema. *Environ. Res.* 33(2):473–496.

Campbell, E. J. M. 1958. The respiratory muscles and the mechanics of breathing. London: Lloyd-Luke, Ltd.

Chen, J. C., Brenner, M., Katie, F. E., Yoong, B., Budd, M., Gassel, A., Waite, T. A., Milliken, J., Huh, J., Wang, N. S., McKenna, R., Gelb, A., Wilson, A. F., and Berns, M. W. 1998. An animal model for lung volume reduction therapy of pulmonary emphysema. *J. Invest. Surg.* 11(2):129–137.

Collie, D. D. 1994. Exponential analysis of the pressure-volume characteristics of ovine lungs. *Respir. Physiol.* 95(3):239–247.

Collie, D. D., Watt, N. J., Warren, P. M., Begara, I., and Lujan, L. 1993. Lung compliance, lung volume and transfer factor for carbon monoxide in anaesthetised sheep: Normal values and reproducibility of measurements. *Res. Vet. Sci.* 55(2):137–143.

Corne, S., and Anthonisen, N. R. 2002. *Lung function testing in chronic obstructive pulmonary disease.* Hamilton: B.C. Decker, Inc.

Criner, G. J., Cordova, F. C., Furakawa, S., Kuzma, A. M., Travaline, J. M., Leyenson, V., and O'Brien, G. M. 1999. Prospective randomized trial comparing bilateral lung volume reduction surgery to pulmonary rehabilitation in severe chronic obstructive pulmonary disease. *Am. J. Respir. Crit. Care Med.* 160(6):2018–2027.

D'Angelo, E. 1976. Effect of papain-induced emphysema on the distribution of pleural surface pressure. *Respir. Physiol.* 27(1):1–20.

DuBois, A., Botelho, S., Bedell, G., Marshall, R., and Comroe, J. H., Jr. 1956. A rapid plethysmographic method for measuring thoracic gas volume: a comparison with a nitrogen dilution method for measuring functional residual capacity in normal subjects. *J. Clin. Invest.* 35:322–326.

Geddes, D., Davies, M., Koyama, H., Hansell, D., Pastorino, U., Pepper, J., Agent, P., Cullinan, P.,

MacNeill, S. J., and Goldstraw, P. 2000. Effect of lung-volume-reduction surgery in patients with severe emphysema. *N. Engl. J. Med.* 343(4):239–245.

Gibson, G. J., Pride, N. B., Davis, J., and Schrater, R. C. 1979. Exponential description of the static pressure-volume curve of normal and diseased lungs. *Am. Rev. Respir. Dis.* 120(4):799–811.

Hachenberg, T., Wendt, M., Schreckenberg, U., Meyer, J., Hermeyer, G., Muller, K. M., and Lawin, P. 1989. Single breath N_2 washout in papain-induced pulmonary emphysema. *Intens. Care Med.* 15(5):308–313.

Haddad, A. G., Pimmel, R. L., Scaperoth, D. D., and Bromberg, P. A. 1979. Forced oscillatory respiratory parameters following papain exposure in dogs. *J. Appl. Physiol.* 46(1):61–66.

Hantos, Z., Daroczy, B., Csendes, T., Suki, B., and Nagy, S. 1990. Modeling of low-frequency pulmonary impedance in dogs. *J. Appl. Physiol.* 68(3):849–860.

Hubmayr, R. D., Farkas, G. A., Tao, H. Y., Sieck, G. C., and Marguilies, S. S. 1993. Diaphragm mechanics in dogs with unilateral emphysema. *J. Clin. Invest.* 91(4):1598–1603.

Huh, J., Brenner, M., Chen, J. C., Yoong, B., Gassel, A., Katie, F., Milliken, J. C., McKenna, R., Jr., Fischel, R. J., Gelb, A., and Wilson, A. F. 1998. Changes in pulmonary physiology after lung volume reduction surgery in a rabbit model of emphysema. *J. Thorac. Cardiovasc. Surg.* 115(2):328–334; discussion 334–335.

Ingenito, E. P., Reilly, J. J., Mentzer, S. J., Swanson, S. J., Vin, R., Keuhn, H., Berger, R. L., and Hoffman, A. 2001. Bronchoscopic volume reduction: A safe and effective alternative to surgical therapy for emphysema. *Am. J. Respir. Crit. Care Med.* 164(2):295–301.

Janoff, A., Chanana, A. D., Joel, D. D., Susskind, H., Laurent, P., Yu, S. Y., and Dearing, R. 1983. Evaluation of the urinary desmosine radioimmunoassay as a monitor of lung injury after endobronchial elastase instillation in sheep. *Am. Rev. Respir. Dis.* 128(3):545–51.

Johanson, W. G., Jr., and Pierce, A. K. 1972. Effects of elastase, collagenase, and papain on structure and function of rat lungs in vitro. *J. Clin. Invest.* 51(2):288–293.

Kaczka, D. W., Ingenito, E. P., Body, S. C., Duffy, S. E., Mentzer, S. J., DeCamp, M. M., and Lutchen, K. R. 2001. Inspiratory lung impedance in COPD: effects of PEEP and immediate impact of lung volume reduction surgery. *J. Appl. Physiol.* 90(5):1833–1841.

Karlinsky, J. B., and Snider, G. L. 1978. Animal models of emphysema. *Am. Rev. Respir. Dis.* 117(6): 1109–1133.

Karlinsky, J. B., Snider, G. L., Franzblau, C., Stone, P. J., and Hoppin, F. G., Jr. 1976. In vitro effects of elastase and collagenase on mechanical properties of hamster lungs. *Am. Rev. Respir. Dis.* 113(6): 769–777.

Klassen, T., Thurlbeck, W. M., and Berend, N. 1981. Correlation between lung structure and function in a canine model of emphysema. *J. Appl. Physiol.* 51(2):321–326.

Kuhn, C. 3rd, Slodkowska, J., Smith, T., and Starcher, B. 1980. The tissue response to exogenous elastase. *Bull. Eur. Physiopathol. Respir.* 16(suppl.):127–139.

Lucey, E. C., Snider, G. L., and Javaheri, S. 1982. Pulmonary ventilation and blood gas values in emphysematous hamsters. *Am. Rev. Respir. Dis.* 125(3):299–303.

Lutchen, K. R., and Gillis, H. 1997. Relationship between heterogeneous changes in airway morphometry and lung resistance and elastance. *J. Appl. Physiol.* 83(4):1192–1201.

Lutchen, K. R., Yang, K., Kaczka, D. W., and Suki, B. 1993. Optimal ventilation waveforms for estimating low-frequency respiratory impedance. *J. Appl. Physiol.* 75(1):478–488.

Lutchen, K. R., Greenstein, J. L., and Suki, B. 1996. How inhomogeneities and airway walls affect frequency dependence and separation of airway and tissue properties. *J. Appl. Physiol.* 80(5):1696–1707.

Marco, V., Meranze, D. R., Yoshida, M., and Kimbel, P. 1972. Papain-induced experimental emphysema in the dog. *J Appl Physiol* 33(3):293–9.

Margulies, S. S., Schriner, R. W., Schroeder, M. A., and Hubmayr, R. D. 1992. Static lung-lung interactions in unilateral emphysema. *J. Appl. Physiol.* 73(2):545–551.

Mauderly, J. L. 1984. Respiratory function responses of animals and man to oxidant gases and to pulmonary emphysema. *J. Toxicol. Environ. Health* 13(2–3):345–361.

Meyer, J., Hachenberg, T., Hermeyer, G., Lippert, G., Schreckenberg, U., Struckmeier, O., and

Wendt, M. 1991. [The effect of PEEP-ventilation on gas exchange and airway closure in experimental pulmonary emphysema]. *Anaesthetist* 40(3):166–171.
Mink, S. 1984. Expiratory flow limitation and the response to breathing a helium–oxygen gas mixture in a canine model of pulmonary emphysema. *J. Clin. Invest.* 73:1321–1334.
Mundie, T. G. D. K. T., and Lautchik, M. 1992. Relationship of functional residual capacity to various body measurements in normal sheep. *Lab. Anim. Sci.* 42(6):589–592.
Niewoehner, D. E., and Kleinerman, J. 1973. Effects of experimental emphysema and bronchiolitis on lung mechanics and morphometry. *J. Appl. Physiol.* 35(1):25–31.
Oliven, A., Supinski, G.S., and Kelsen, S. G. 1986. Functional adaptation of diaphragm to chronic hyperinflation in emphysematous hamsters. *J. Appl. Physiol.* 60(1):225–231.
Petak, F., Hantos, Z., Adamicza, A., and Daroczy, B. 1993. Partitioning of pulmonary impedance: Modeling vs. alveolar capsule approach. *J. Appl. Physiol.* 75(2):513–521.
Port, C. D., Ketels, K. V., Coffin, D. L., and Kane, P. 1977. A comparative study of experimental and spontaneous emphysema. *J. Toxicol. Environ. Health* 2(3):589–604.
Pushpakom, R., Hogg, J. C., Woolcock, A. J., Angus, A. E., Macklem, P. T., and Thurlbeck, W. M. 1970. Experimental papain-induced emphysema in dogs. *Am. Rev. Respir. Dis.* 102(5):778–789.
Rodarte, J., and Rehder, K. 1986. Dynamics of respiration. *Handbook of physiology*, ed. A. P. Fishman, vol. 3, pp. 131–293. Bethesda, MD: American Physiologic Society.
Salazar, E., and Knowles, J. 1964. An analysis of pressure volume characteristics of the lungs. *J. Appl. Physiol.* 19(1):97–104.
Shiraishi, K., Fukuda, Y., Nakagawa, J., and Motomiya, M. 1989. [Correlation between the function and structure in papain-induced emphysema in dogs]. *Kokyu To Junkan* 37(11):1203–1208.
Snider, G. L., Lucey, E. C., and Stone, P. J. 1986. Animal models of emphysema. *Am. Rev. Respir. Dis.* 133:149–169.
Snider, G. L., Martorana, P. A., Lucey, E. C., and Lungarella, G. 2002. Animal models of emphysema. In *Chronic obstructive lung diseases,* eds. N. Voelkel and W. MacNee, vol. 1, pp. 237–256. Hamilton: B. C. Decker.
Snider, G. L., and Sherter, C. B. 1977. A one-year study of the evolution of elastase-induced emphysema in hamsters. *J. Appl. Physiol.* 43(4):721–729.
Sullivan, K. J., Fournier, M., and Lewis, M. I. 1998. Respiratory work in elastase treated hamsters. *Respir. Physiol.* 114(2):133–142.
Susskind, H., Chanana, A. D., Joel, D. D., Brill, A. B., Janoff, A., Som, P., and Oster, Z. H. 1984. Acute response to elastase in sheep lungs measured with Ga-67. *J. Nucl. Med.* 25(12):1310–1316.
Szelenyi, I., and Marx, D. 2001. Animal models of chronic obstructive pulmonary disease. *Arzneimittelforschung* 51(12):1004–1014.
Takaro, T. 1978. Physiologic effects of the position of the body in experimental unilateral emphysema. *Chest* 74(1):72–76.
Thomas, A. J., Supinski, G. S., and Kelsen, S. G. 1986. Changes in chest wall structure and elasticity in elastase-induced emphysema. *J. Appl. Physiol.* 61(5):1821–1829.
Verbeken, E. K., Cauberghs, M., Mertens, I., Lauweryns, J. M., and Van de Woestijne, K. P. 1992. Tissue and airway impedance of excised normal, senile, and emphysematous lungs. *J. Appl. Physiol.* 72(6):2343–2353.
Wright, J. L., and Churg, A. 1992. Cigarette smoke causes physiologic and morphologic changes of emphysema in the guinea pig. *Am. Rev. Respir. Dis.* 142:1422–1428.